Scatterfield Microscopy, Review of Techniques that Push the Limit of Optical Defect Metrology

Rick Silver
Group Leader, Surface and Nanostructure Metrology Group
National Institute of Standards and Technology

Bryan Barnes	**Defect Modeling and Analysis**
Martin Sohn	**193 nm Scatterfield Microscope**
Francois Goasmat	**Programming and Simulation**
Hui Zhou	**Simulation Engine**
Andras Vladar	**SEM Measurements**
Abraham Arceo	**SEMATECH, Wafer development**

NIST
National Institute of Standards and Technology
U.S. Department of Commerce

- ITRS metrology roadmap shows defect inspection as red, without known solutions in just two years. We are working with the major manufacturers and suppliers to evaluate and develop new techniques to meet these needs.

- The main challenge: to measure very small, nanometer scale features over large patterned areas in manufacturing. There is a fundamental incompatibility between throughput and resolution.

- Optical methods offer unparalleled throughput with tremendous sensitivity. Spatial frequency modulation of the illumination and collection fields can be tailored to enhance optical defect signals.
  - Further gains can be achieved at shorter wavelengths
  - The arrayed and directional aspects of current and future device fabrication are well suited to engineered optical fields

Outline

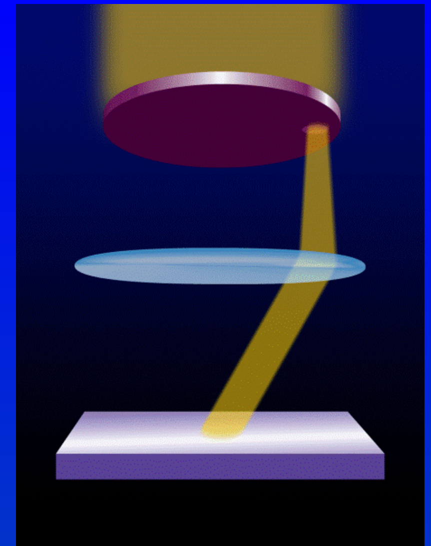

- Scatterfield Optical Microscopy
- Simulations
  - Quantitative validation
  - 3-D Patterned Defects
- Angle and Polarization Enhanced Sensitivity
  - Wavelength optimization
- Multi-dimensional Defect Detection
  - Rigorously using three-dimensional focus information
- Future Directions in Inspection
- Conclusions

Source and Collection Optimization for Arrayed Patterns

Scatterfield Microscopy

- **Optical microscopy**
  - High magnification, image forming optics
- **Source optimization, frequency control, and structured illumination**

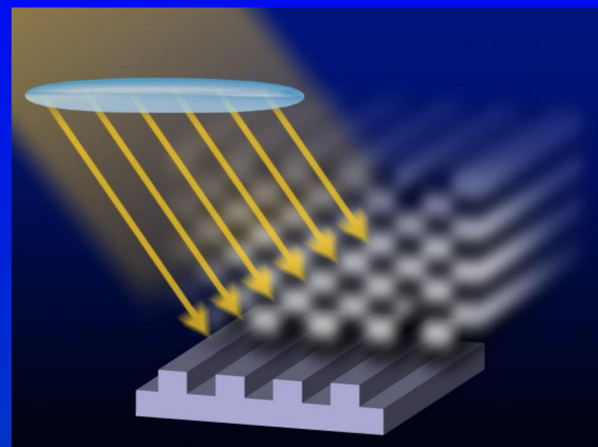

R. Silver *et al.*, Proc. SPIE 5752, 67-79 (2005).

line-to-line

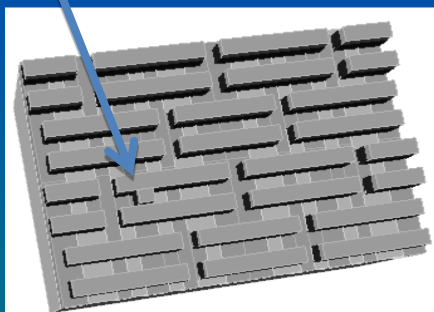

end-to-end

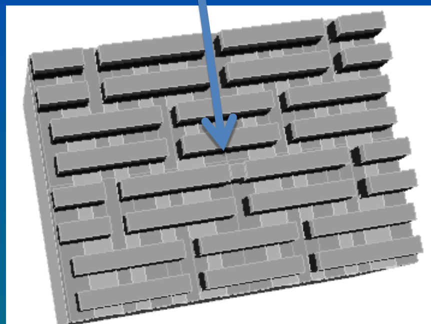

Optimizing optical defect inspection using:

- wavelength
- polarization
- spatial frequency
- focus position
- control coherence

Simulation Studies to Assess Trends in Detectability

Highly directional bridge defects

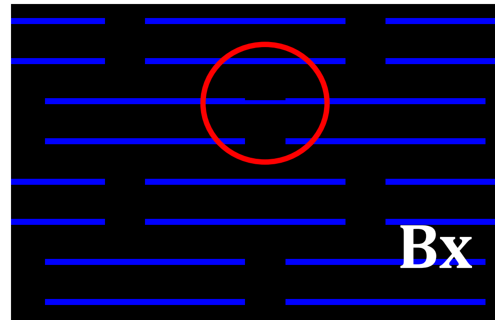

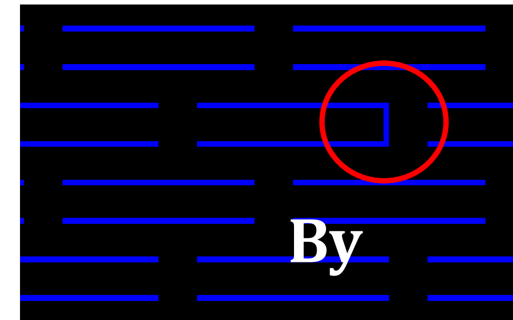

Defect Metric Definition

- **Random and correlated noise, with 3σ = 2% of mean(I_{ref}), is added to each difference image.**
- **The defect metric is the absolute intensity sum of the pixels with intensities greater than 4σ for regions larger than a specified area.**

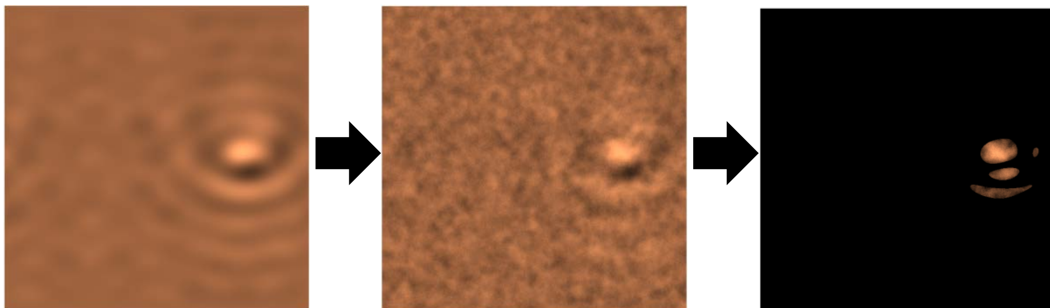

Definition of axes

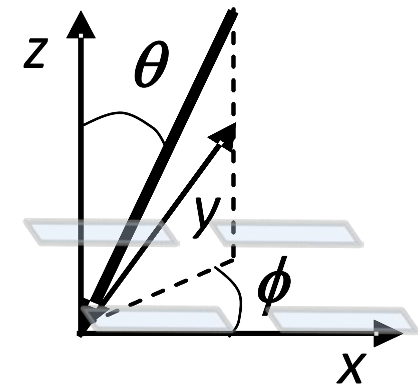

2.16 μm x 2.16 μm FDTD domain (3x9 unit cell rep.)
grid size = 3 nm, λ = 193 nm

Defect Simulation Details

- **Three-dimensional simulations of structures are performed on defects from the 22 nm to defects below 10 nm.**
  - Finite-difference time-domain (FDTD)
    - In-house code
  - RCWA code
    - In-house but primarily used for 2-D modeling
  - Finite Element Method (FEM)
    - Commercially available code
    - Integral equation solver (in-house)
- **Results are subtracted for die-to-defect comparisons**

Theory-to-experiment comparisons for defect metrology.

Defect “By”

Each image normalized individually.

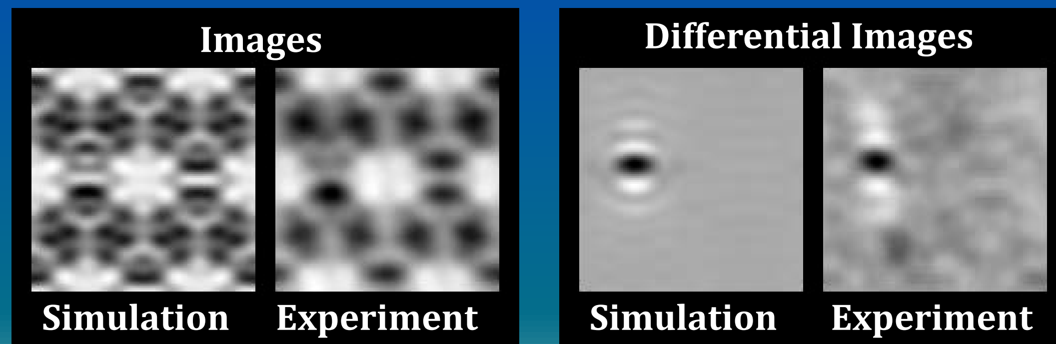

Developing Accurate Simulation Methods: Advanced Tool Characterization

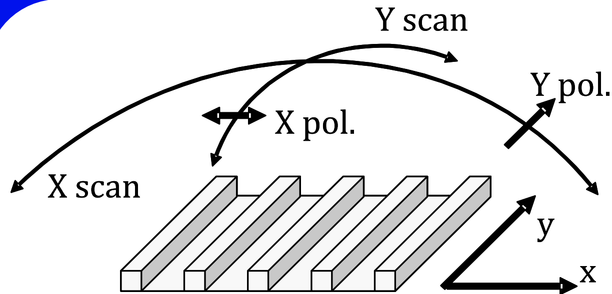

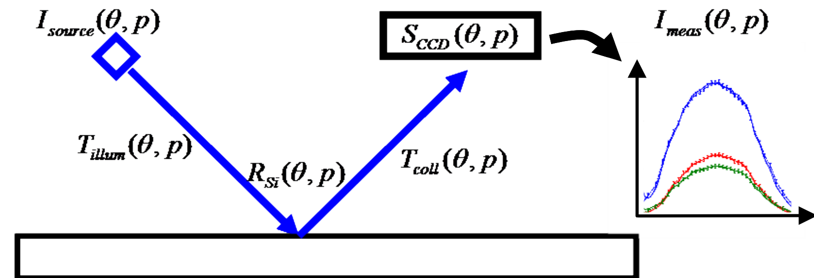

$$I_{source}(\theta, p) \times T_{illum}(\theta, p) \times R_{Si}(\theta, p) \times T_{coll}(\theta, p) \times S_{CCD}(\theta, p) = I_{meas}(\theta, p),$$

$$T_{0-order} = I_{meas}(\theta, p) / R_{Si}(\theta, p) \Rightarrow R_{sample}(\theta, p) = I_{sample}(\theta, p) / T_{0-order}$$

Illumination Path

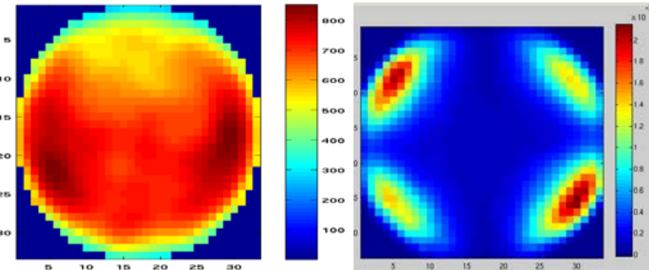

$I_{PD}(\theta, \varphi, ps)$

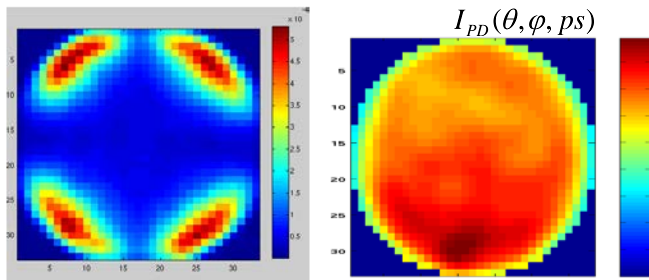

$I_{PD}(\theta, \varphi, sp)$

Complete Path

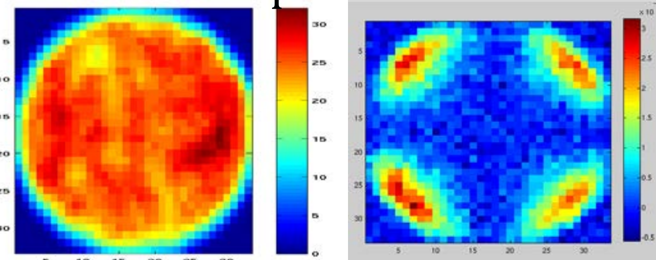

$I_{CCD}(\theta, \varphi, ps)$

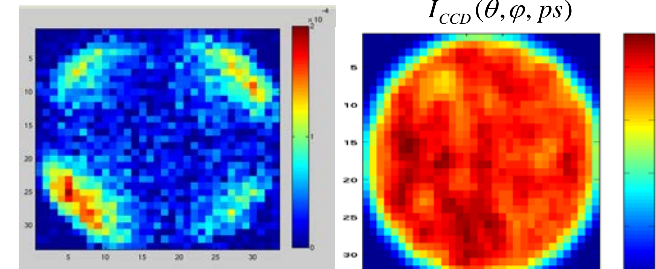

$I_{CCD}(\theta, \varphi, sp)$

50 nm pillar array, 175 nm pitch at λ=450 nm

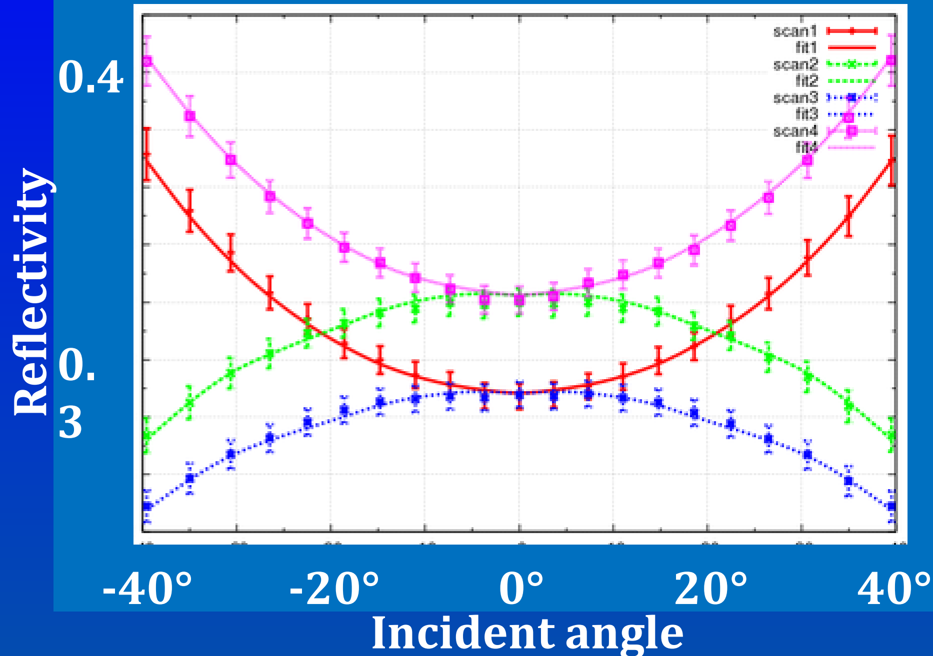

Incident angle

OCD parameterization

	a	σ_a
middle	45.27 nm	2.77 nm
δ	26.27 nm	6.61 nm
height	82.12 nm	5.99 nm
aspect	1.19	0.01

OCD with with δ_{AFM} and h_{AFM}

	a	σ_a
middle	48.91 nm	0.89 nm
δ	18.17 nm	2.63 nm
height	73.84 nm	1.78 nm
aspect	1.19	0.01

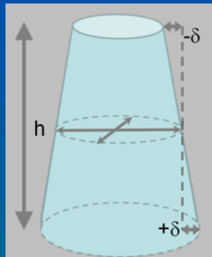

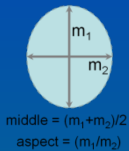

middle = $(m_1+m_2)/2$
aspect = (m_1/m_2)

AFM values

middle = 55.3 nm ± 2.4 nm
δ = 18.7 nm ± 4.2 nm
height = 72.8 nm ± 2 nm

Right tables show measurements with hybrid metrology embedding AFM.

Fitting Optimized Targets for sub-20 nm CD Metrology

- Sets of nominally 14nm, 16 nm, and 18 nm lines were fabricated by SEMATECH based on NIST designs.
- Targets are Si on Si with a thin conformal oxide. Wafers fabricated using ebeam litho.
- Line extensions were included to facilitate AFM measurements. Note AFM measurements may have a bias compared to dense area optical measurements.
- **Current target sizes as small as 1.75 μm x 6 μm.**

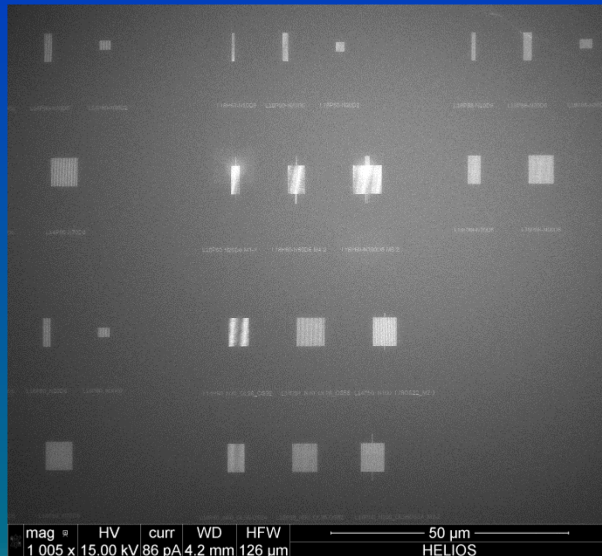

Overview of patterned area

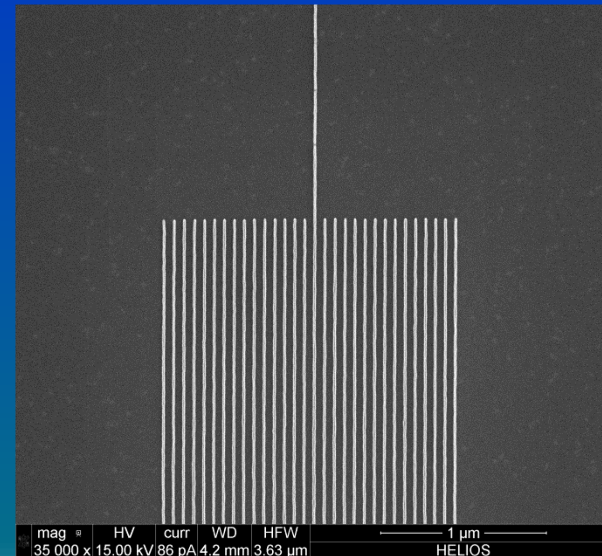

30 line array

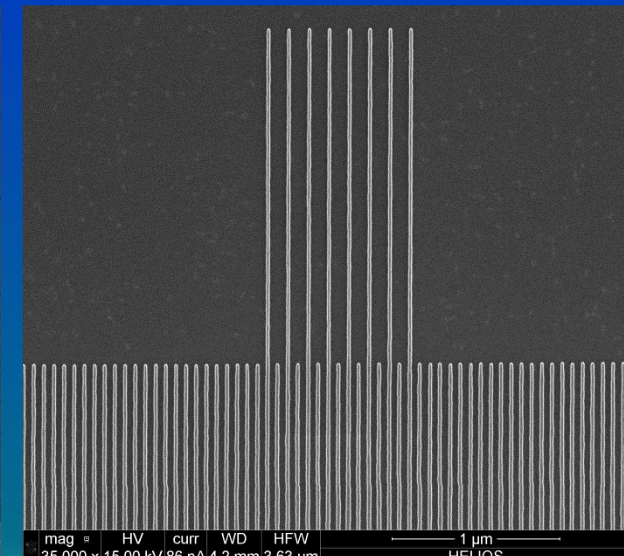

100 line array

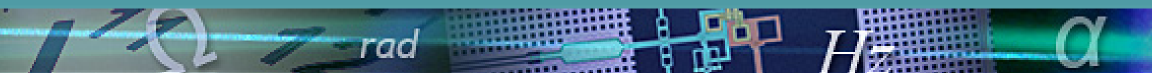

Data Fitting for L14P60 30-line Dense Array

SEM example

X-polarized light

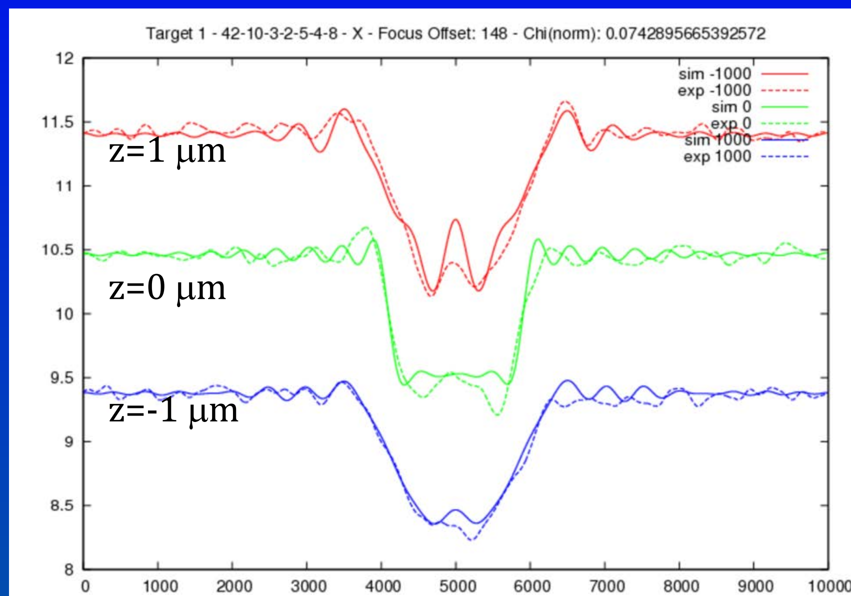

Y-polarized light

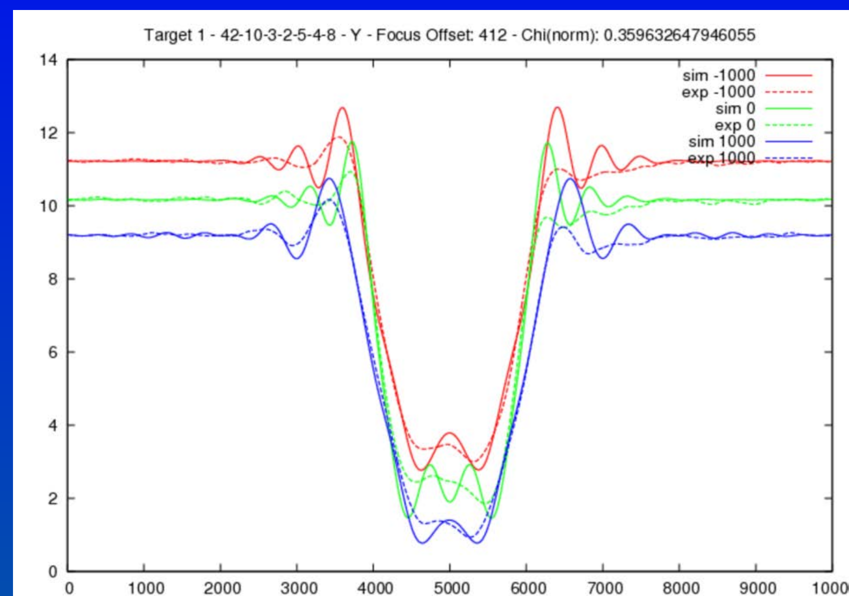

Best Fits:
- 5 nm SiO2 cap
- 45nm Si height
- 7 nm at 1.0h
- 11 nm at 0.8h
- 14 nm at 0.5h
- 16 nm at 0.3h
- 24 nm at base

AFM data:
- 45nm Si height
- 13 nm at 0.8h
- 16 nm at 0.5h
- 18 nm at 0.2

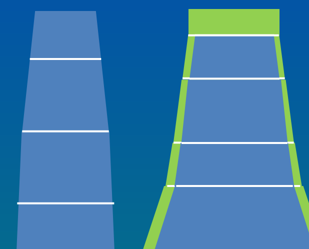
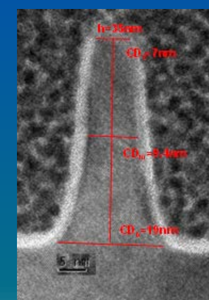

Parametric model

Theory to Experiment Fits: 100-line Dense Array

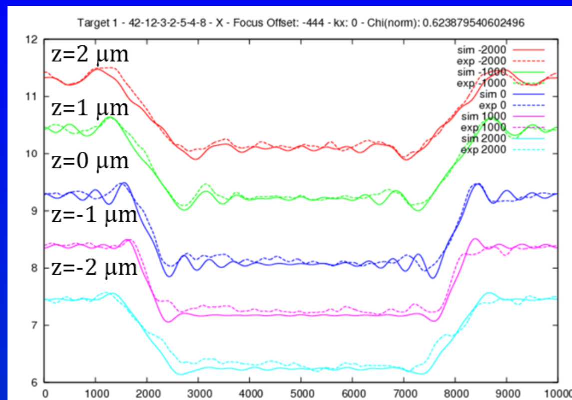

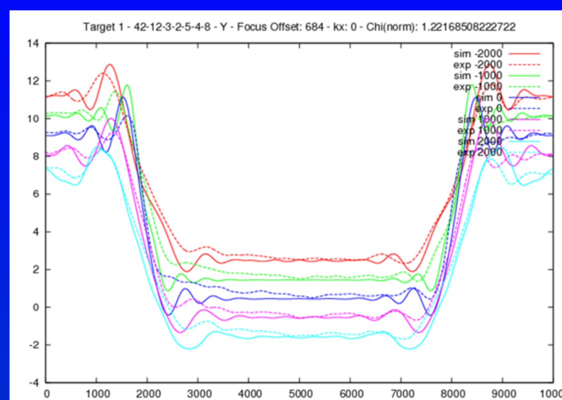

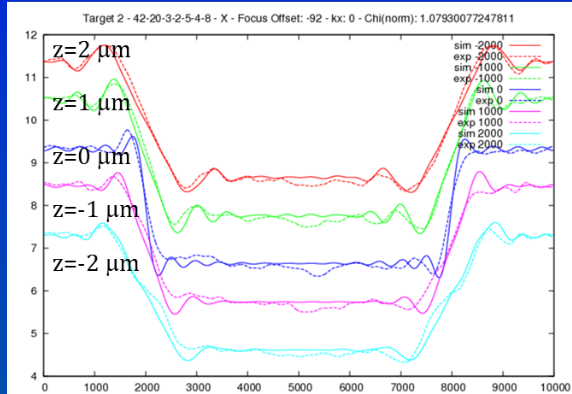

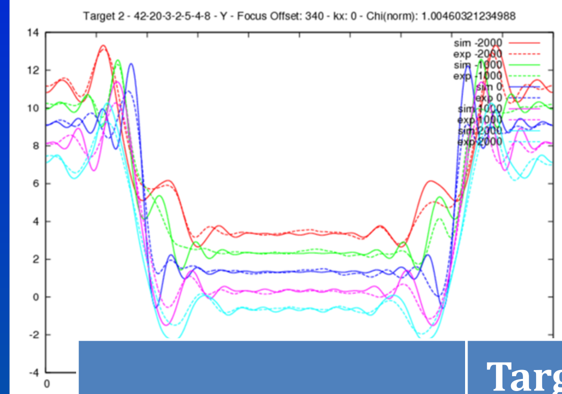

- Fits shown on left with uncertainties in table below.
- Target 1 has width and height floated with 2 oxide capping thicknesses.
- Target 2 has same plus top width floated.

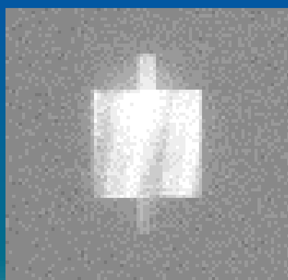

	Target 1	Target 2
Height (nm)	42 ± 0.024	45 ± 0.123
CD [1.0 h] (nm)	9	17
[0.8 h](nm)	13	21 ± 0.047
[0.5 h] (nm)	16 ± 0.017	24 ± 0.210
[0.3 h] (nm)	18	26
[0.0 h] (nm)	26	34

Simulation Study: Polarization and Angle Dependence

15 nm Bridge Defects

TE polarization – s pol. TM Polarization – p pol.

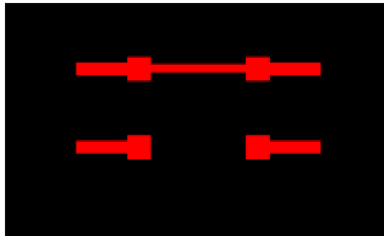

Bx

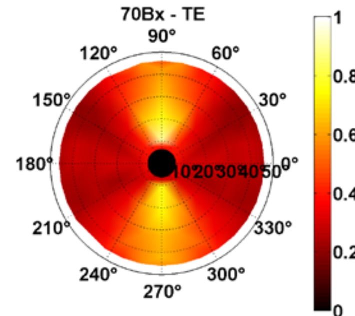

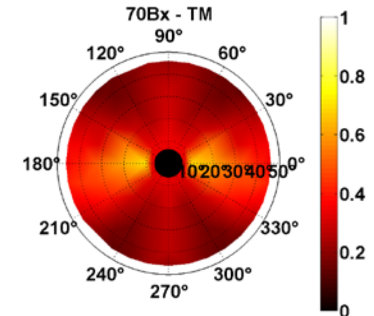

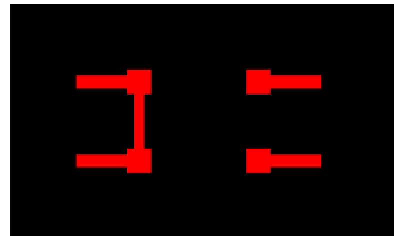

By

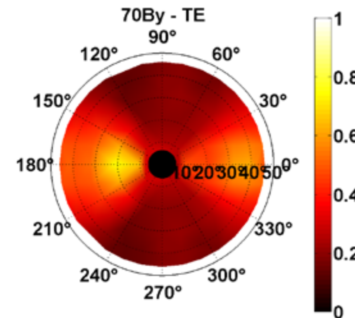

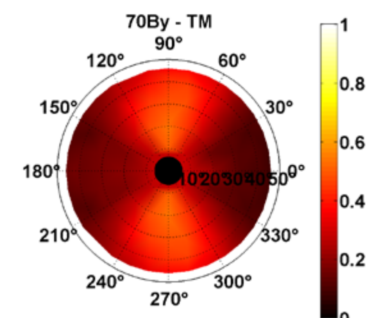

- These highly directional bridges with narrow widths are optimally detected at particular combinations of θ and ϕ.
- As the direction of the bridge changes 90°, the optimal combinations of θ and ϕ rotate by 90°.
- Detectability for the By defect is not symmetric for TE polarization.

Simulation Study: Polarization and Angle-Resolved Detection
8 nm Bridge Defects

Bx

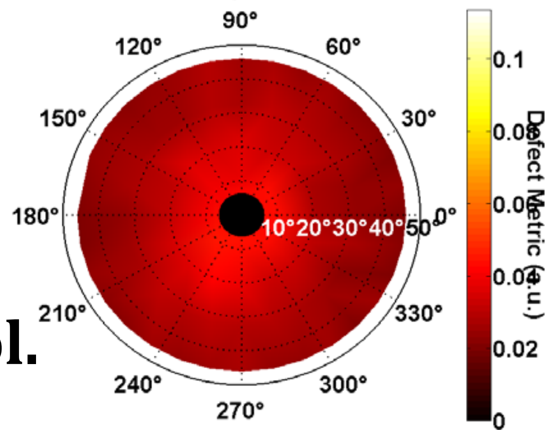

X pol.

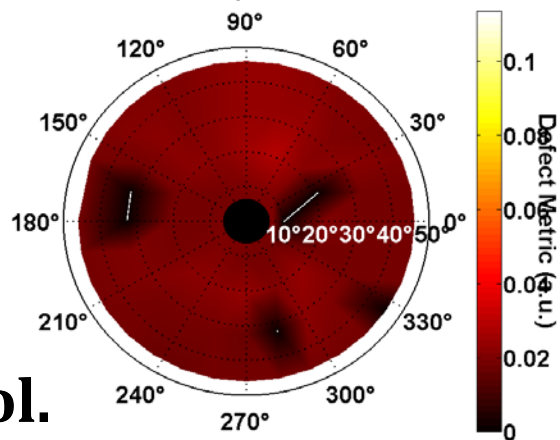

Y pol.

By

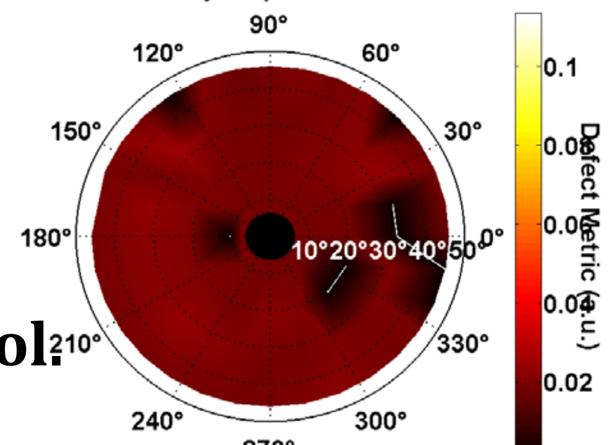

X pol.

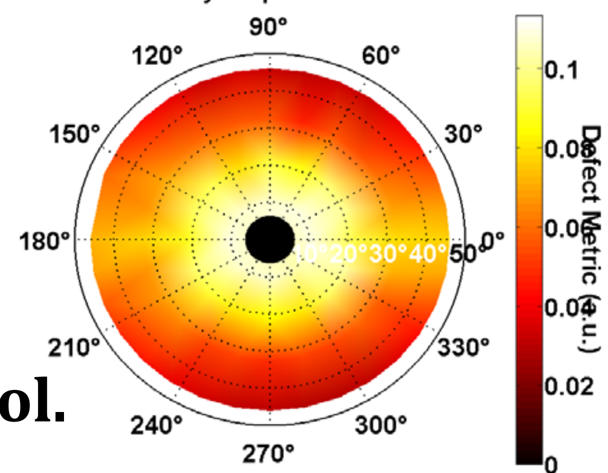

Y pol.

- **These highly directional bridges are sensitive to polarization and to a lesser extent, the polar angle, θ. The azimuthal angle ϕ has a modest effect.**

Experiment: 193 nm Laser Optical Metrology System

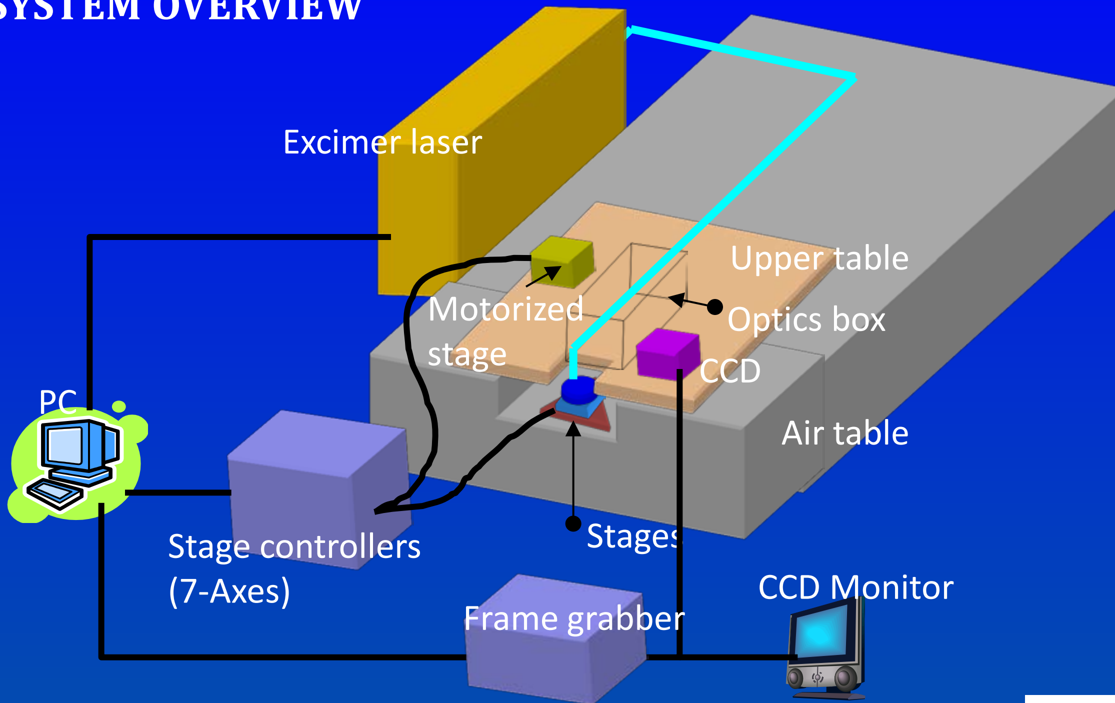

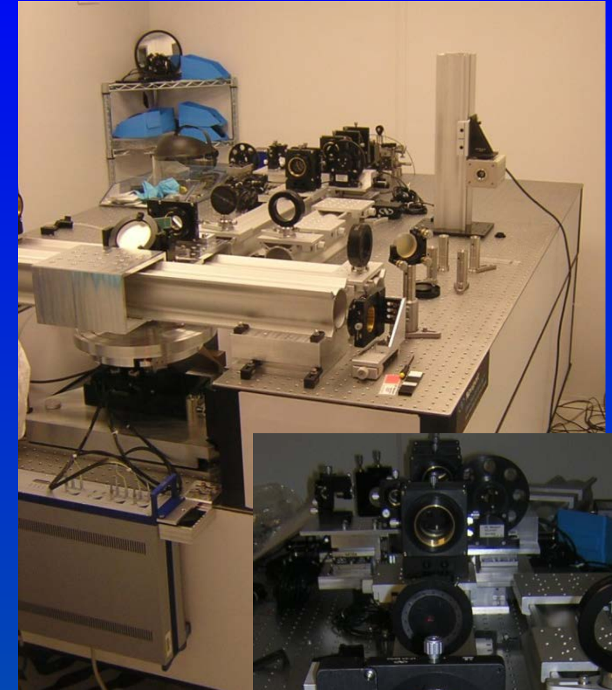

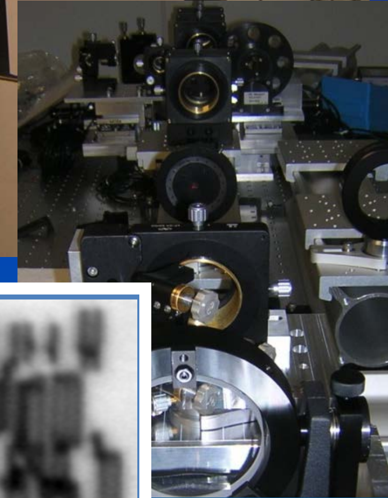

Angular Scan Mode

- Nearly plane wave illumination
- Pinhole apertures 20 um~1500 um
- Control of illumination angle, polarization, and phase

Full Field Modification Mode

- Modify distribution of illumination
- Motorized rotating aperture holder
- Modify spatial intensity distribution
- Control polarization state

Major upgrades underway.

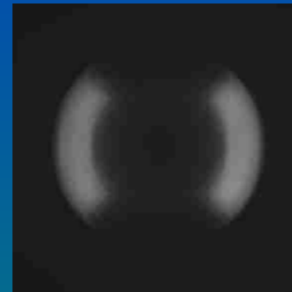

Fourier image of dipole illumination

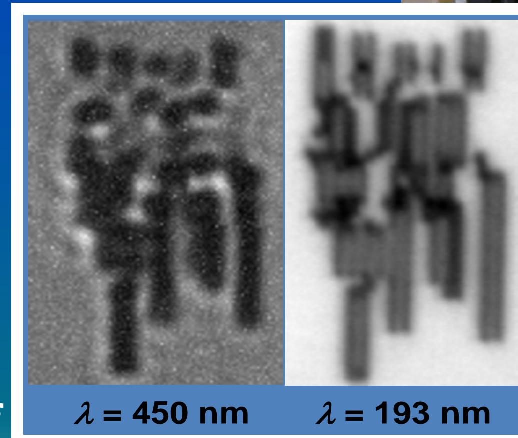

Theory-to-experiment Comparison at λ = 193 nm

Lower examples show defects 15 nm in size based on reference measurements.

Defect	Illumination		Images		Differential Images	
	Aperture	Polarization	Simulation	Experiment	Simulation	Experiment

A160

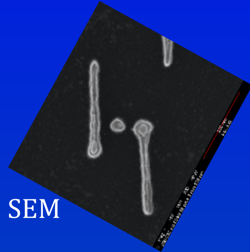

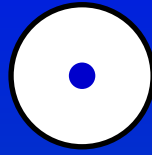

Full-field

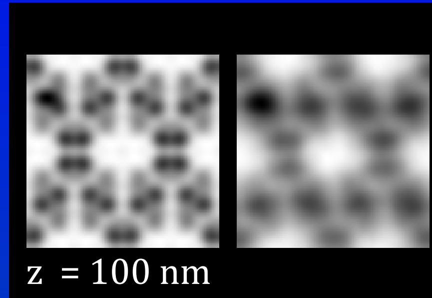

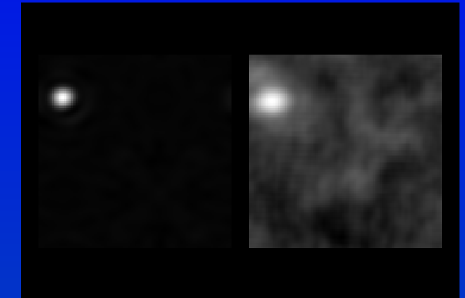

Bx60

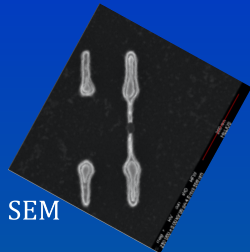

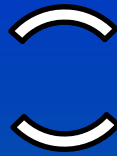

Dipole

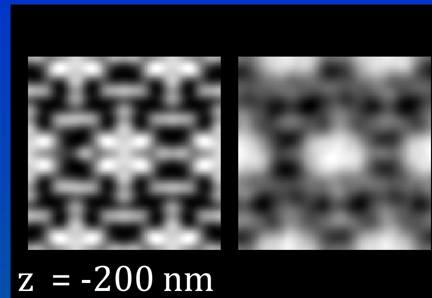

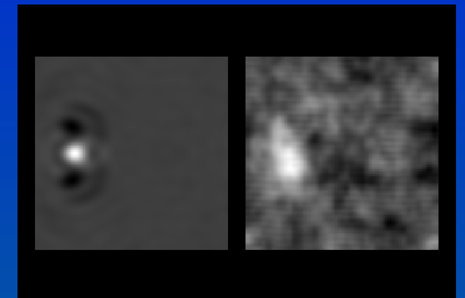

By60

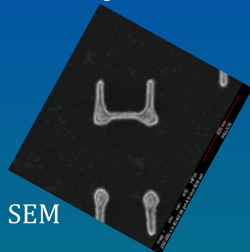

Dipole

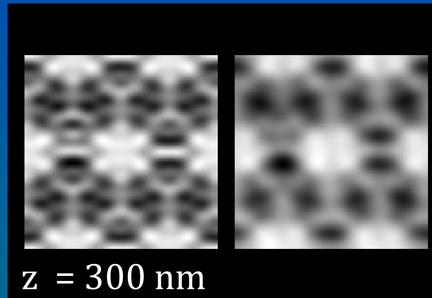

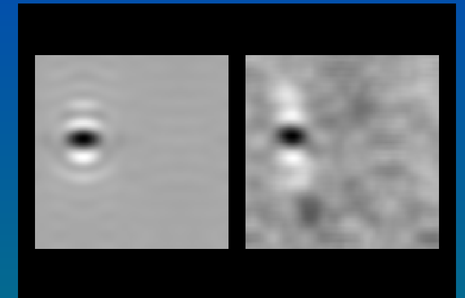

- **Simulations qualitatively trend with experimental results.**
- **Clearly, not all aspects of the microscope are accounted for here.**

Using all the Three Dimensional Data for Inspection

- Capturing images through focus not only finds a best focus for observing defectivity but also provides additional correlated data.
- Two-dimensional treatments of the data cannot fully utilize this information.

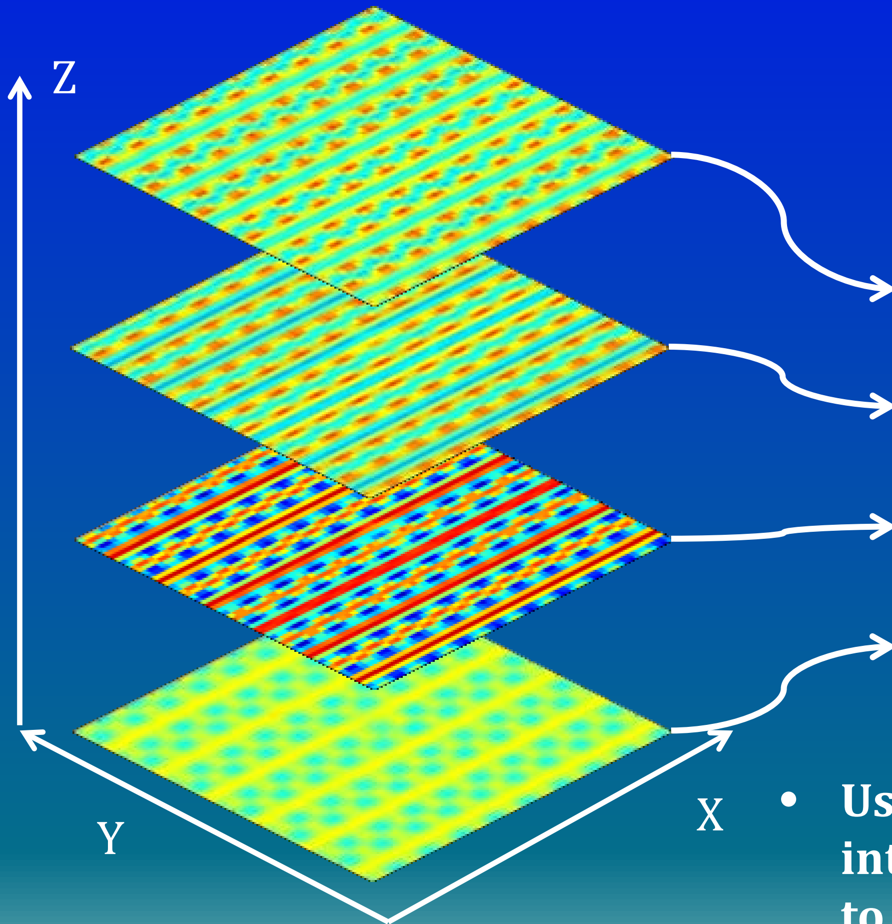

- Each image is *m* x *n* pixels which are typically square.

Image simulation of dipole illumination with X polarization on a 8 nm Bx defect at λ=193 nm.

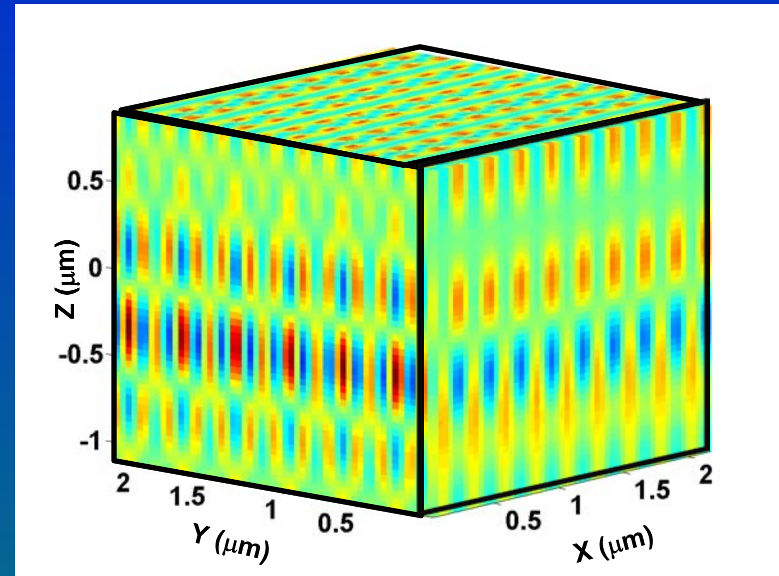

- Using matched focus positioning or interpolation, match *xy* pixel pitch to *z* position to form cubic volumetric pixels (voxels).

Using all the Three Dimensional Data for Inspection

- As with all defect simulations, noise should be added to benchmark detectability.
- Subtraction of the two volumes leads directly to a difference volume.

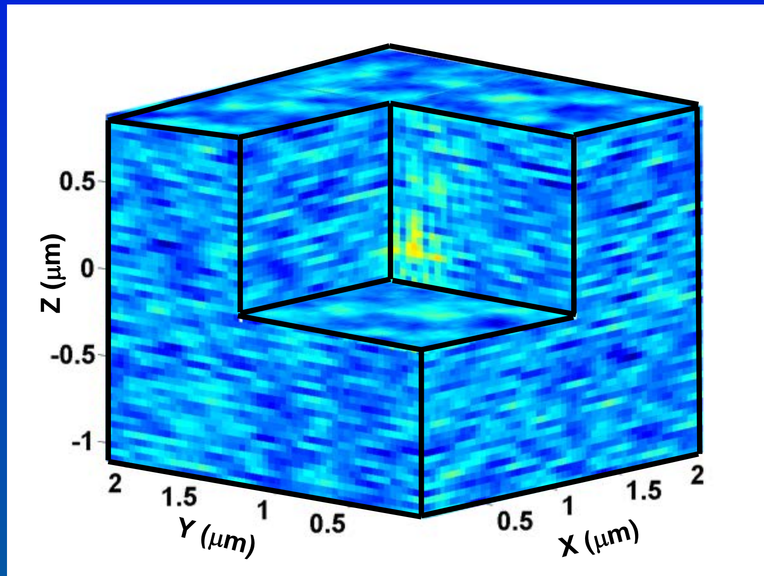

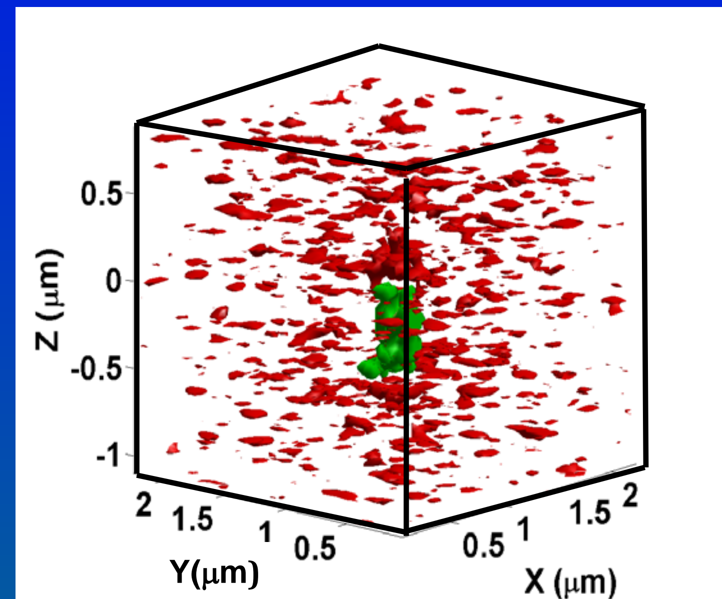

- With this 3-D matrix, we are now in a position to exploit
  - 3-D continuity, 3-D filtering, 3-D thresholding,
  - As well as employing standard methods over the full volume.

Experiments on the 9 nm node SEMATECH IDA at λ = 193 nm

Additional Experimental Intensity Processing Steps

- Fourier intensity filtering
  - Operates on the defect and reference volumes
- 3-D correlation of volumes

- *Note*: shift between "defect" and "reference" image is < 1 μm, thus two defect signatures are measured.

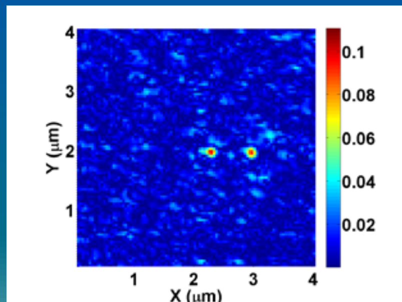

The 9 nm node IDA

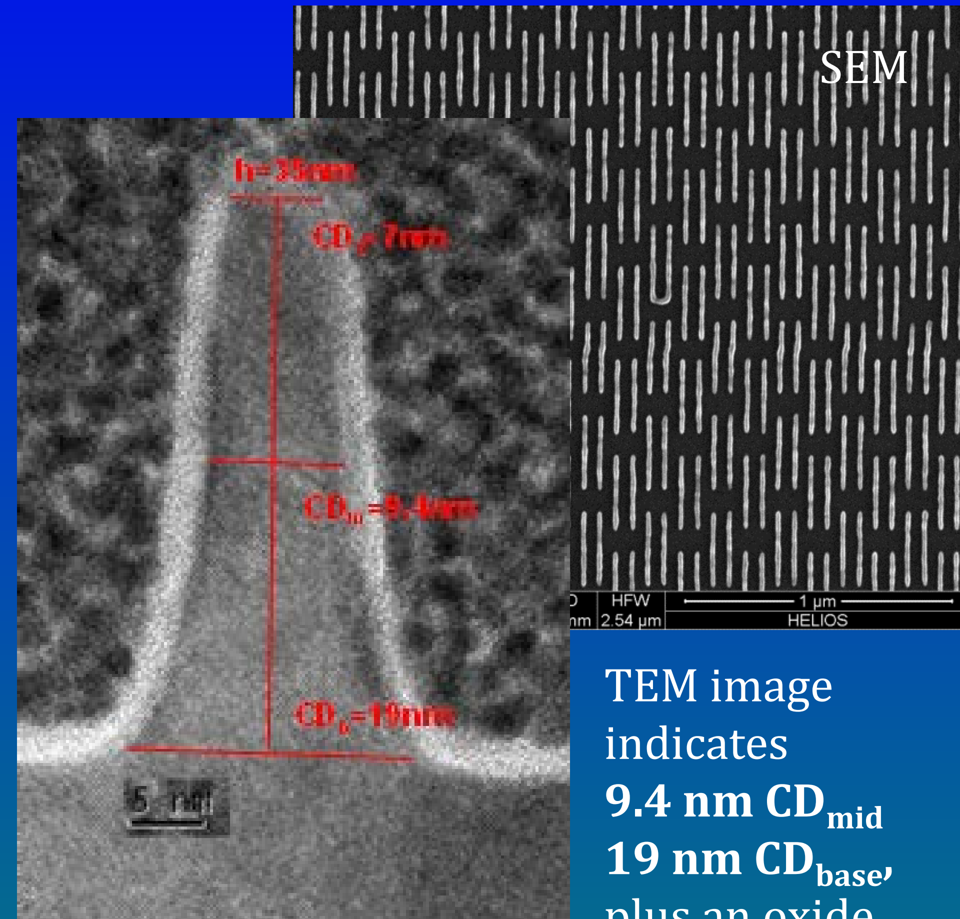

TEM of subsequent printing of this array

TEM image indicates **9.4 nm CD_{mid}** **19 nm CD_{base},** plus an oxide.

Experimental Validation: J defect – Y pol. , λ = 193 nm

J defect schematic

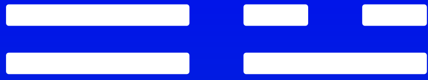

The defect volume can be visualized as a
- 2D slice
- 3D isometric view
- XY projection
- XZ projection
- YZ projection

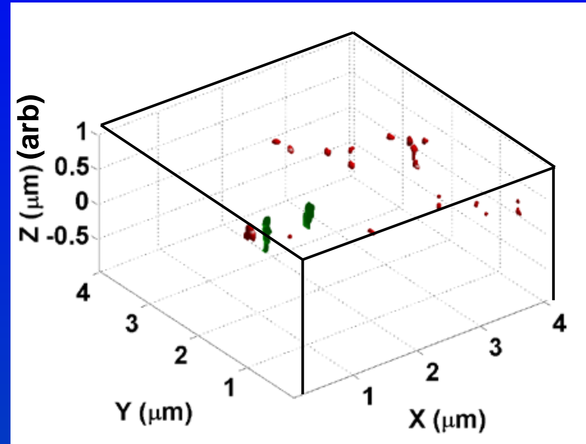

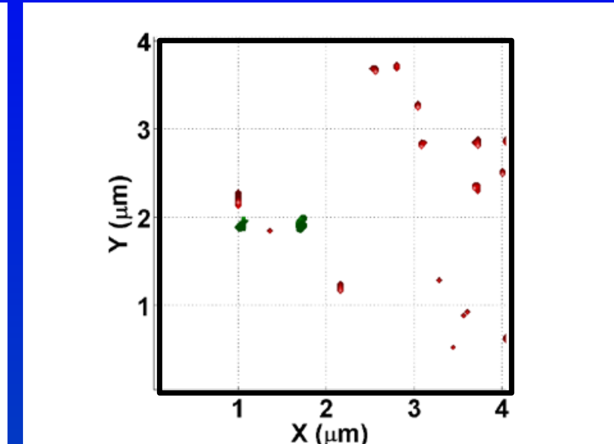

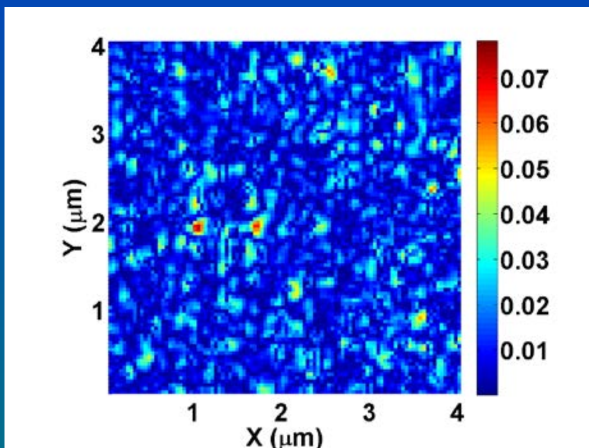

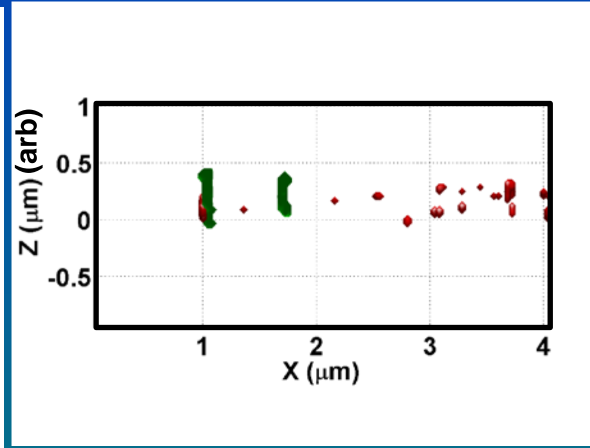

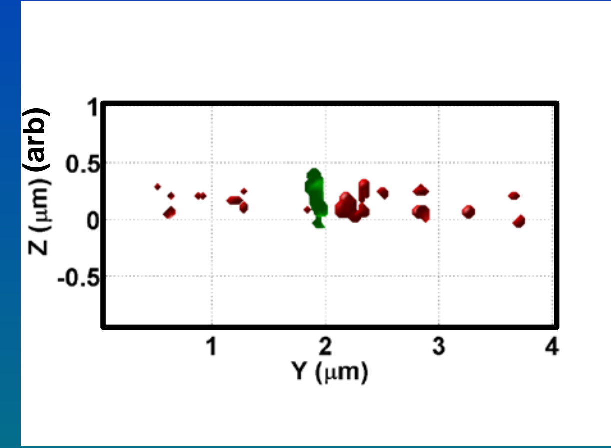

Experimental Validation: By defect – Y pol. , λ = 193 nm

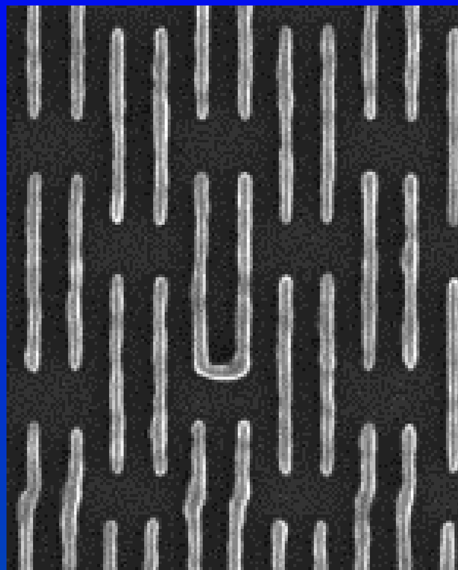

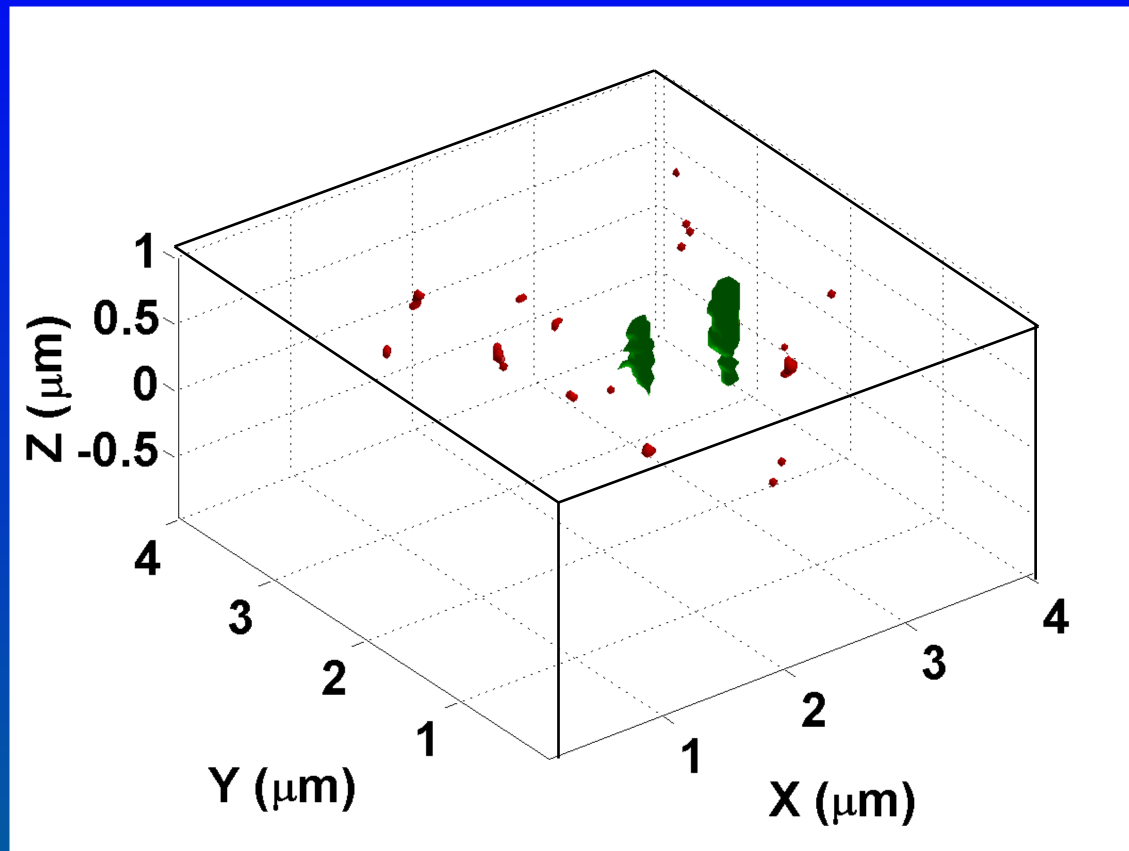

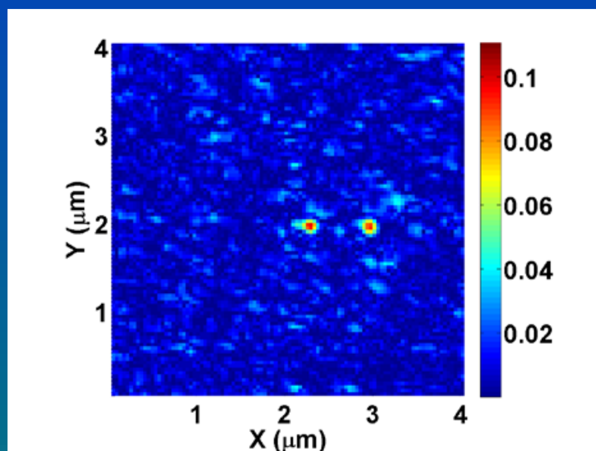

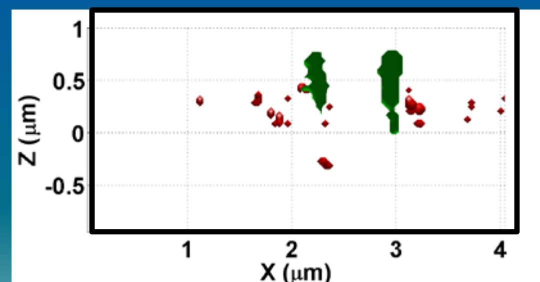

XZ projection

Volumetric-based Focus Metric

Defect J Die (3,3) Pol Y

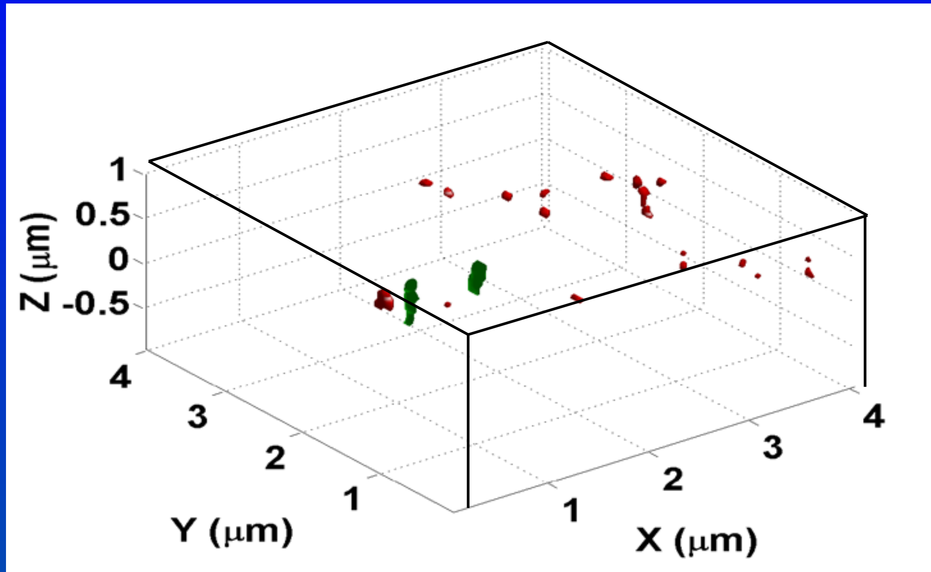

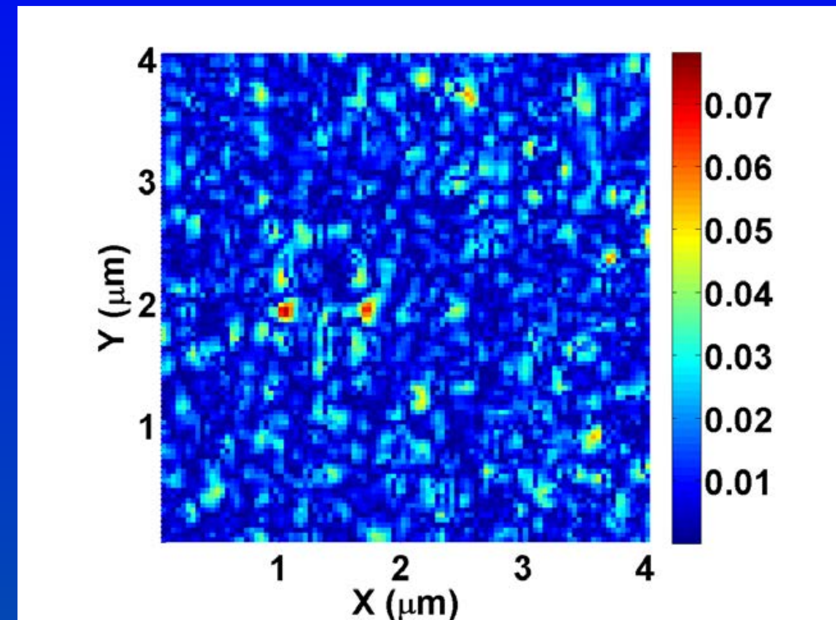

In this example, a five-fold increase in sensitivity is observed

	Area (pixels^2)	Integrated Intensity (a.u.)
2-D best image	8	0.50
3-D flatten Y	42	6.03
3-D flatten X	42	

Summary of Volumetric-based Focus Metric

- **The addition of the focus-resolved data increases the defect sensitivity using an area-based defect metric by about a factor of five or more for at least one of the two 3-D projections used.**

Area ($pixels^2$)

	2nd Die, "Bx" *Y* pol. 1.33 DR	1st Die, "By" *Y* pol. 0.45 DR	2nd Die, "By" *X* pol. 0.89 DR	1st Die, "J" *Y* pol. 1.55 DR
2-D Best Image	21	12	5	8
3-D, Flatten *x*	88	72	27	42
3-D, Flatten *y*	96	69	18	42

- **The improvement in sensitivity between the 2-D and 3-D results varies with defect type, ranging by a factor of 7.5 up to a factor of 14.9 .**

Integrated Intensity (a.u.)

<table>
<tr><th></th><th>2nd Die, "Bx"
Y pol.
1.33 DR</th><th>1st Die, "By"
Y pol.
0.45 DR</th><th>2nd Die, "By"
X pol.
0.89 DR</th><th>1st Die, "J"
Y pol.
1.55 DR</th></tr>
<tr><td>2-D Best Image</td><td>2.30</td><td>0.87</td><td>1.29</td><td>0.50</td></tr>
<tr><td>3-D, Flatten *x*</td><td rowspan="2">31.49</td><td rowspan="2">12.96</td><td rowspan="2">9.79</td><td rowspan="2">6.03</td></tr>
<tr><td>3-D, Flatten *y*</td></tr>
</table>

Angle and Focus Resolved Detection: Dipole Illumination

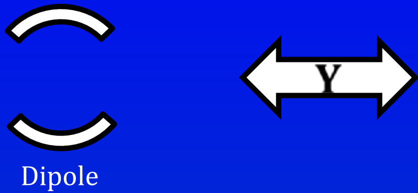

Data taken with polarization along the bridge direction.

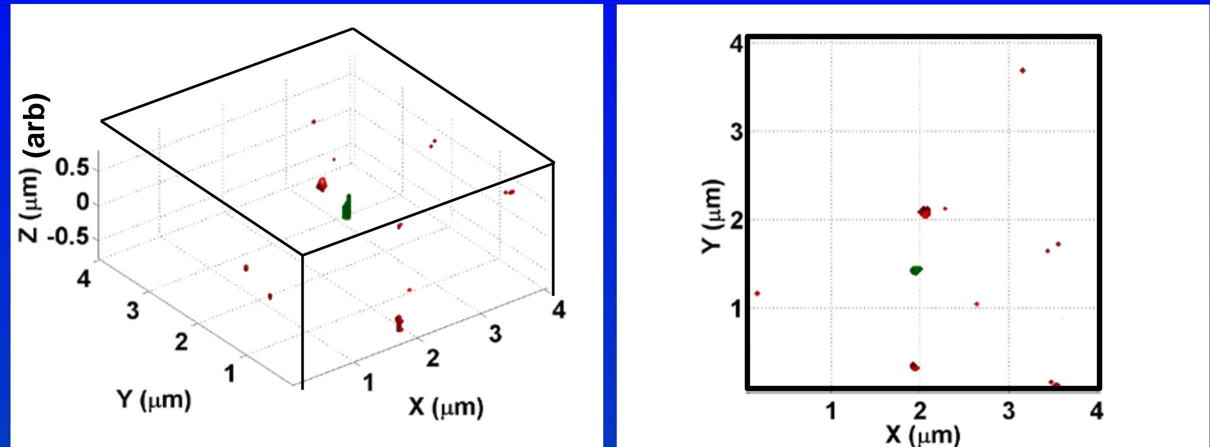

By defect – Y pol.

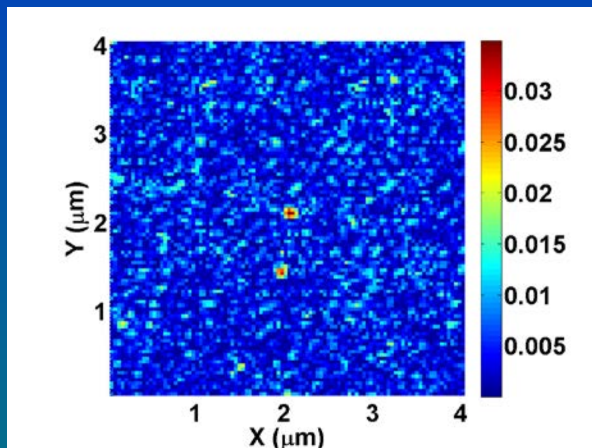

	Area (pixels^2)	Integrated Intensity (a.u.)
2-D best image	4	0.010
3-D flatten Y	15	0.074
3-D flatten X	15	0.076

New Directions: Potential Gains in Coherent Imaging

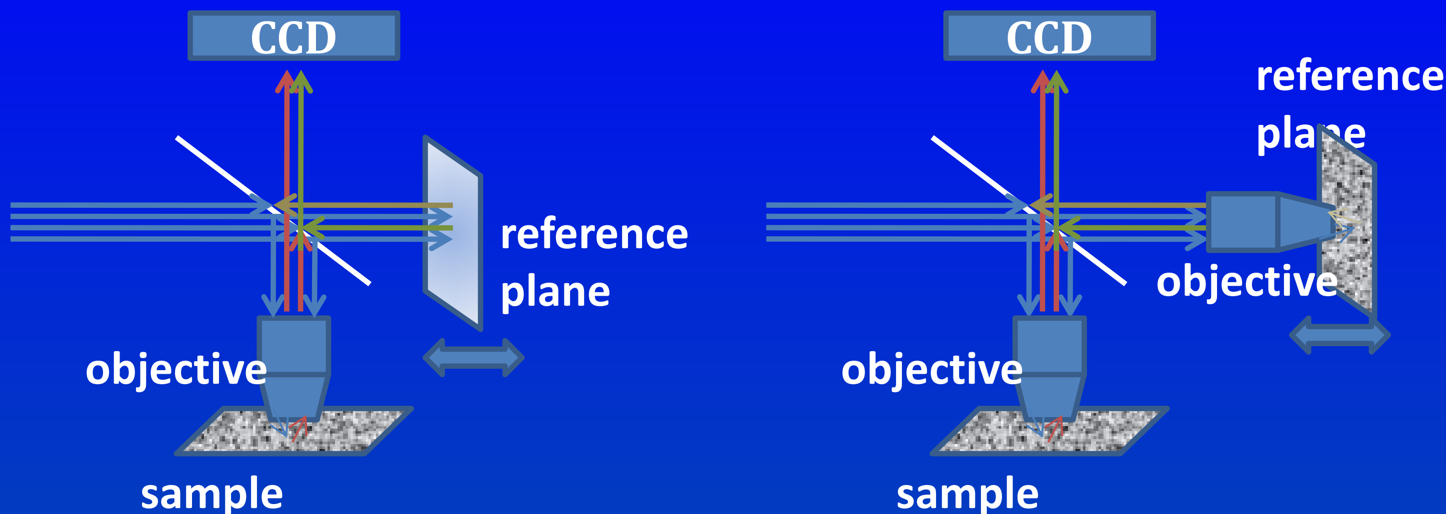

Interference microscopy using simple reference plane. Difference intensity images simulated using the FEM model for 22nm.

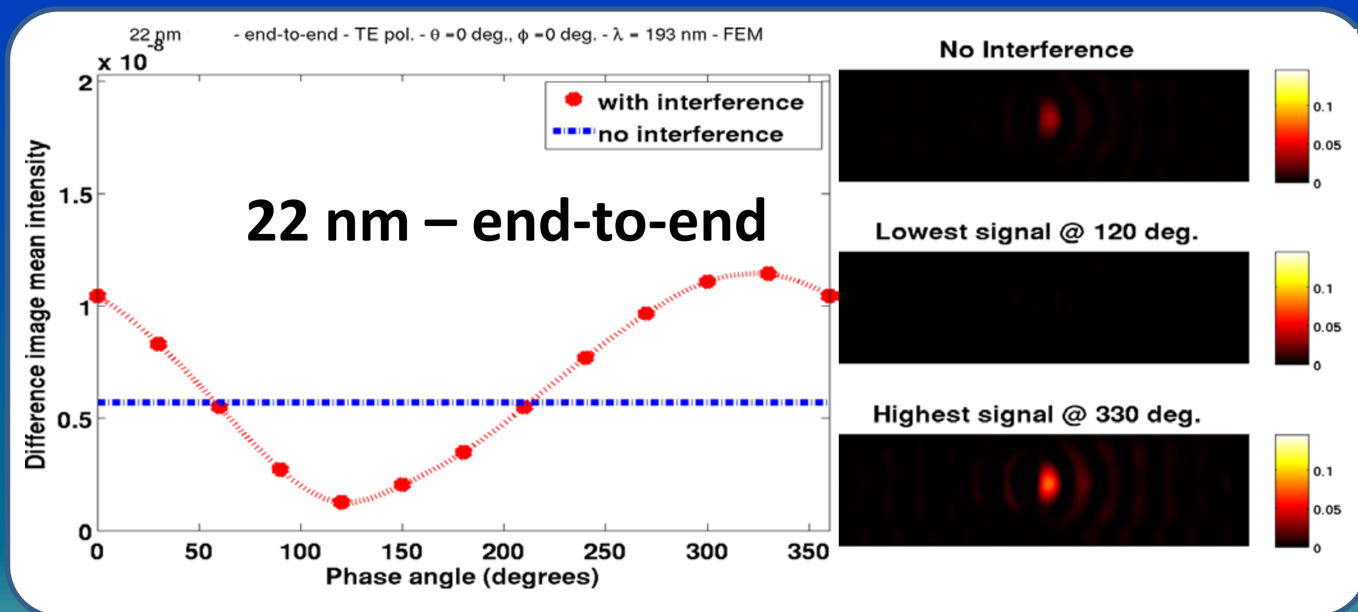

Scatterfield Microscopy for Improved Defect Detection

- Simulations demonstrate clear optimal combinations of angular illumination and polarization.
- Experimental verification of simulation trends has been observed with qualitative theory-to-experiment matching for a variety of apertures, polarizations, and defect types.
- A clear, quantifiable gain in sensitivity of up to five was demonstrated using three-dimensional focus information through multi-dimensional defect detection.
  - This approach allows the full range of 3-D filters, continuity, and algorithms to be explored.
- New directions in coherent imaging and Fourier frequency control were described.